JPE 18-3-7

https://doi.org/10.6113/JPE.2018.18.3.714
ISSN(Print): 1598-2092 / ISSN(Online): 2093-4718

Wide-range Speed Control Scheme of BLDC Motor Based on the Hall Sensor Signal

Dong-Hee Lee†

†Department of Mechatronics Engineering, Kyungsung University, Busan, Korea

Abstract

This paper presents a wide-range speed control scheme of brushless DC (BLDC) motors based on a hall sensor with separated low- and normal-speed controllers. However, the use of the hall sensor signal is insufficient to detect motor speed in the low-speed region because of low sensor resolution and time delay. In the proposed method, a micro-stepping current control method according to the torque angle variation is presented. In this mode, the motor current frequency and rotating angle are determined by the reference speed without the actual speed fed by the hall sensor. The detected torque angle is used to adjust the current value in a limited band to control the current value in accordance with the load. The torque angle is detected exactly at the changing point of the hall sensor signal. The rotor can follow the rotating flux with the variable torque angle. In a normal speed range, the conventional vector control scheme is used to control the motor current with a PI speed controller using the hall sensor. The torque characteristics are analyzed on the basis of the back EMF and current shape. To adopt the vector control scheme, the continuous rotor position is estimated by the measured speed and hall sensor position. At the mode changing point between low and normal speed range, the proper initial current command and reference rotor position are calculated. The calculated current command can reduce the torque ripple during transient mode. The proposed method is simple but effective in extending the speed control range of a conventional BLDC motor with hall sensor without the need for a high-resolution encoder. The effectiveness of the proposed method is verified by various experiments on a practical BLDC motor.

Key words: Brushless DC motor, Micro-step torque angle, Speed control, Wide speed range

I. INTRODUCTION

Brushless DC (BLDC) motors are widely used in home appliances, such as blenders, crude liquid machines, and industrial applications, due to their high power and torque characteristics and excellent control performance while being low cost [1]-[5].

The speed and torque control of BLDC motors can be implemented by using hall sensor signals and a phase current in a conventional application. Unlike an encoder, the hall sensor signal can only determine the electric rotor position in 60° intervals. Thus, accurate speed detection during the controllable sampling period in the low speed is difficult. Depending on the application, the general current control period is 50–200 μs and the speed detecting and control period is 200 μs–10 ms [6], [7]. In the low-speed region of BLDC motors, the measurable period of the hall sensor signal is more than 100 ms, and the load can suddenly change during this period. A slight voltage change by PWM control can also result in a high-speed ripple in the low speed range. Given these problems, the speed control of BLDC motors has been mainly used in the medium speed to high speed range only [8], [9]. For high-performance control systems, the permanent magnet synchronous motor (PMSM) with an encoder is suitable due to its torque characteristics and speed sensor resolution. However, the cost of PMSM with an encoder is unsuitable for adoption in conventional applications. The proposed method can extend the speed control range of a conventional BLDC motor with a low-cost hall sensor without any additional cost or high-resolution encoder.

In previous studies, an observer is used to estimate the practical speed [8], [9]. This method is very useful in low-speed regions with an encoder. However, the actual detected signal of the hall sensor is nearly 1 Hz in the low-speed region. Thus, the observer estimation is not useful in

Manuscript received May 22, 2017; accepted Dec. 13, 2017
Recommended for publication by Associate Editor Zheng Wang.
†Corresponding Author: leedh@ks.ac.kr
Tel: +82-51-663-4693, Fax: +82-51-554-0186, Kyungsung University
Department of Mechatronics Engineering, Kyungsung University

the hall-sensor-based BLDC motor. To implement the proper observer and the online learning model of BLDC motor, a precise rotor position is essential [10], [11]. However, the use of hall sensor signal is insufficient for the conventional observer in the low speed range because of its low resolution and time delay.

In the low speed range, micro-stepping method for the stepping motor is widely used in industrial applications [12]. However, the conventional micro-stepping method is based on the open-loop current control without any position feedback. Thus, the speed ripple and vibration during the phase change are higher than in other motors. When an encoder with high resolution is adopted in the motor, observer technologies can be a useful choice for speed calculation in the low speed range [7]-[9]. Given that observers can be updated in the encoder pulse input, the estimated speed by the observers is very accurate. However, the resolution of the hall sensor is very low. The error of the position is only detected six times per electrical frequency of the BLDC motor. Observers are unsuitable for the low-speed control of hall-sensor-based BLDC motors.

The micro-stepping method with variable current in the low-speed region is proposed in this paper. The vector control with PI speed control scheme is used in the normal speed range. The proposed variable torque angle method can be implemented by the open-loop speed control with a rotating current vector according to the reference speed. The magnitude of the current vector is changed to keep the proper torque angle at any hall sensor changing point in accordance with the load variation. The torque angle between the rotating current vector with the reference speed and the magnitude of the current can produce a suitable torque to keep a constant rotor speed in the low-speed region without speed feedback in the sampling period.

In the normal speed range, the continuous rotor position is estimated by the hall sensor signal and the measured speed by the hall sensor period. The torque of the BLDC motor is controlled by the torque current control in the vector control scheme. This method can guarantee excellent performance in the normal speed range. The initial reference angle for the rotating current vector and the initial torque current reference during the change in mode in the proposed control scheme are presented in detail.

In Section II, the practical problem in the BLDC motor with hall sensor and its torque characteristics are explained. The detailed proposed control scheme is presented in Section III.

II. Speed Control of BLDC Motors

A. Speed Measuring Frequency of BLDC Motors

BLDC motors are generally driven by the two-phase conduction mode according to hall sensor signals. In the two-phase conduction mode, the DC current flows into both phase windings at every sequence. The actual speed of the BLDC motor is calculated by the hall sensor signal frequency and period [6].

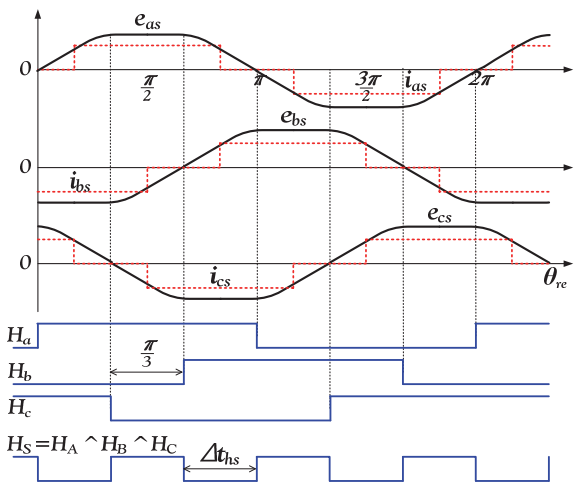

Fig. 1. Back EMF and hall sensor signals of BLDC motor.

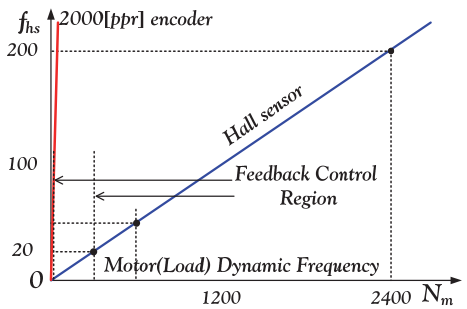

Fig. 2. Measurable frequency of sensor in accordance with speed.

Fig. 1 shows the hall sensor signals and back EMF of a BLDC motor with an ideal phase current. As shown in the figure, the electrical speed of the motor can be derived by the time duration of the combinational signal of the hall sensor as follows:

$$\omega_{re} = \frac{\pi}{3 \cdot \Delta t_{hs}}, \tag{1}$$

From Equation (1), the measurable signal frequency can be determined as follows:

$$f_{hs} = \frac{1}{2 \cdot \Delta t_{hs}}, \tag{2}$$

This measurable frequency must be faster than the motor dynamics to control the motor speed. However, in a four-pole BLDC motor, the measurable signal frequency is 12 Hz at 120 rpm. The mechanical dynamic frequency of BLDC motors is higher than 10 Hz. Therefore, the normal speed control by the hall sensor signal is difficult to perform under 100–200 rpm owing to the measuring frequency and motor dynamics.

Fig. 2 shows the measurable hall sensor signal according to the actual motor speed in a two-pole BLDC motor. As shown

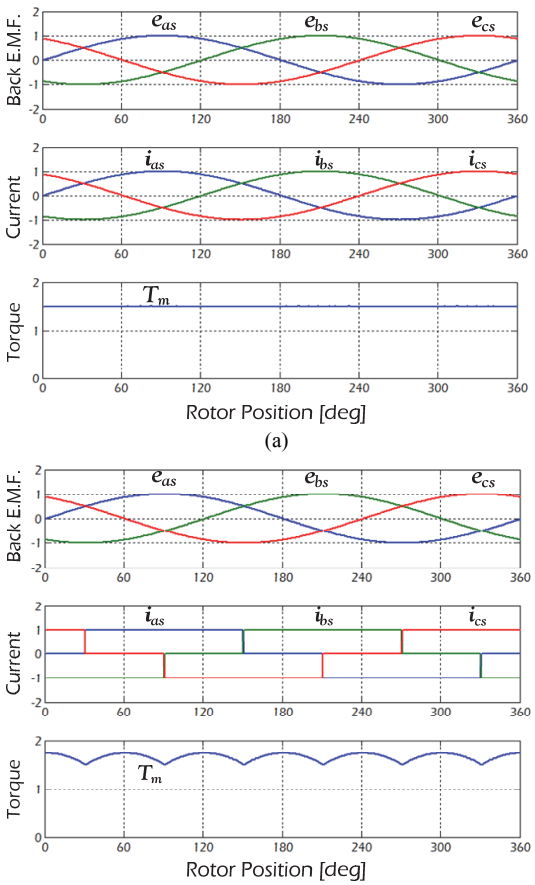

Fig. 3. Torque output of BLDC motor with sinusoidal back EMF. (a) Ideal sine wave current (three-phase conduction mode). (b) Ideal DC current (two-phase conduction mode).

in the figure, the practical controllable region by the hall sensor feedback is limited by the motor and load dynamic frequency. When the motor and load dynamic frequency are faster than the operating speed and hall sensor signal frequency, the speed cannot be controlled by the sensor signal. In a precise encoder, the feedback frequency in accordance with the speed is very fast and the feedback controllable speed is very low at approximately 1 rpm. Thus, the speed control of the BLDC motor with hall sensor is conventionally adopted to be higher than 100–200 rpm.

B. The Output Torque of BLDC Motor

The output torque of BLDC motors is determined by the back EMF and phase current. Some BLDC motors have sinusoidal back EMF while others have trapezoidal back EMF.

The output torque of BLDC motors can be derived by the back EMF and phase currents as follows:

$$T_m = \frac{e_{as}i_{as}+e_{bs}i_{bs}+e_{cs}i_{cs}}{\omega_m}, \quad (3)$$

where e_{as}, e_{bs}, and e_{cs} are the back EMF of each phase; i_{as}, i_{bs}, and i_{cs} are the phase currents; and ω_m is the motor speed.

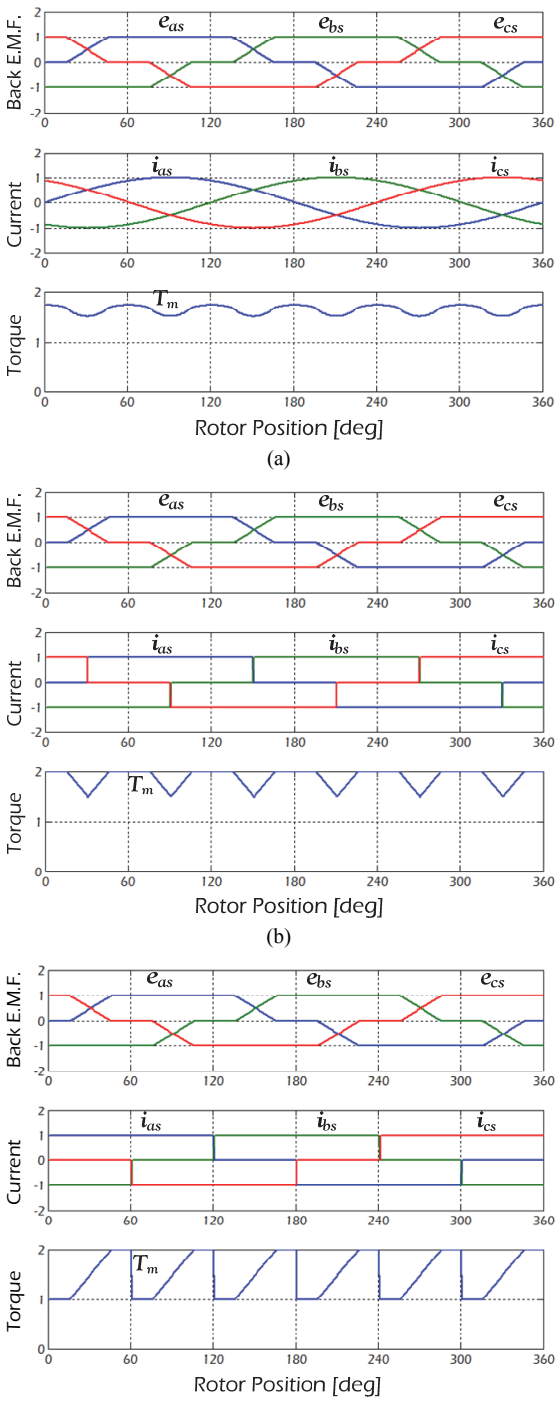

Fig. 4. Torque output of BLDC motor with trapezoidal back EMF. (a) Ideal sine wave current (three-phase conduction mode). (b) Ideal DC current (two-phase conduction mode). (c) Ideal DC current (two-phase conduction mode).

Figs. 3 and 4 show the output torque characteristics of BLDC motor with the sinusoidal and trapezoidal back EMF.

As shown in Fig. 3, the constant output torque can be derived by the ideal sine wave current in accordance with the sinusoidal back EMF model. The torque can be controlled by the vector control method. In the simple two-phase conduction

mode shown in Fig. 3(b), the output torque exhibits ripple due to the back EMF.

In the BLDC motor with trapezoidal back EMF shown in Fig. 4, the output torque presents a ripple for the sine wave current and two-phase DC current mode. However, the sine wave current can reduce the total torque ripple better than the conventional two-phase conduction mode. When the phase current is selected as DC according to the hall sensor, the torque ripple is higher than the ideal case shown in Fig. 4(c). As shown in Figs. 3 and 4, the sine wave current is better than the DC wave current in reducing torque ripple. The three-phase conduction mode is suitable for the low-speed control of the BLDC motor in any case.

In this study, sine wave current control method by the d–q axis is used to reduce the torque ripple.

III. Proposed Control Scheme

A micro-stepping current control method is proposed for the low-speed control of BLDC motor. As previously stated, the use of the feedback control of hall sensor signal is insufficient in the low speed range. Given that motor torque is determined by torque current and torque angle as in (4), the motor speed can be controlled by the torque angle with the torque current of the motor. In field-oriented control, the torque angle is fixed as maximum, and the torque current (q-axis current) is controlled to adjust the motor speed.

$$T_m = K_t \cdot I_m \cdot \sin(\theta_{tm}), \tag{4}$$

where K_t is the torque constant according to the back EMF, I_m is the phase current, and θ_{tm} is the torque angle between the phase current and rotor position.

In the proposed control scheme, the rotating angle of the phase current is determined by motor reference speed, and the motor torque is automatically changed by the torque angle of the motor in accordance with load variation. To improve the efficiency, phase current is controlled by torque angle in every changing point of the hall sensor signal. The phase current is rotated by the reference speed with variable amplitude to produce the proper torque according to the load condition within the safety margin.

Fig. 5 shows the torque control vector in normal and low speed ranges in the proposed control scheme. As shown in the figure, the torque of the BLDC motor is controlled by torque current $I_{m(k)}$, which exhibits an advanced 90° torque angle similar to the vector control in the αβ rotating coordinate. The reference current angle is determined by the actual rotor position $\hat{\theta}_{re(k)}$, which is calculated using the hall sensor signal and measured rotor speed as follows:

$$\widehat{\theta_{re}} = \int p_n \cdot \omega_m \cdot dt + \theta_{hs}(n), \tag{5}$$

where $\theta_{hs}(n)$ denotes an actual rotor position at the signal changing points of hall sensors, and p_n is the number of pole pairs of BLDC motor. In the BLDC motor, the actual

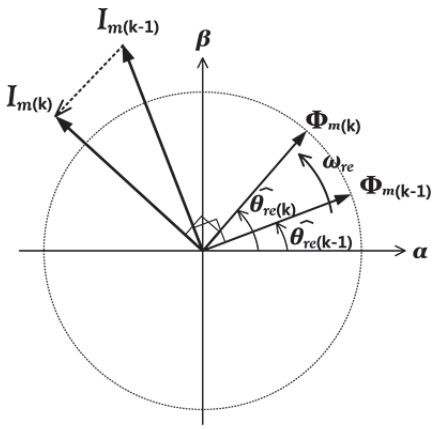

Fig. 5. Torque control of a normal speed range.

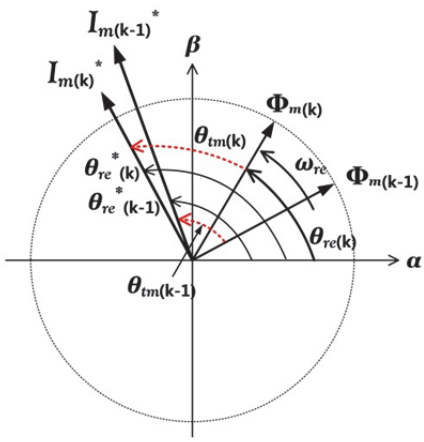

Fig. 6. Torque angle control in the low speed range.

rotor position can be detected by the changing point of the hall sensor signal. Therefore, the estimated continuous position can be derived by the integral of the measured speed. To estimate the continuous rotor position, the frequency of the hall sensor signal must be measurable. In the low-speed region, the frequency of the hall sensor signal is very low and the measured speed is insufficient to accurately control a current vector.

In the normal speed range, the magnitude of the current is determined by the speed error in the speed controller. The speed can be controlled by the conventional speed control scheme, which is designed as PI with anti-windup controller.

Fig. 6 shows the proposed torque angle control scheme in the low speed range. As shown in the figure, the torque current angle is changed by the reference angle θ_{re}^* with the fixed reference speed in αβ rotating surface. The rotating angle of the current can be derived as follows:

$$\theta_{re}^* = \int p_n \cdot \omega_m^* \cdot dt, \tag{6}$$

where ω_m^* is the reference speed. In (6), the actual speed is not used to control the motor speed, and only the current vector is rotating according to the reference speed with micro-step.

In Fig. 6, the actual torque of the motor is determined by the magnitude of the current and torque angle $\theta_{tm(k)}$ between the rotating current vector and the actual rotor vector $\Phi_{m(k)}$, as stated in (4). When the actual current is rotated from $\theta^*_{re(k-1)}$ to $\theta^*_{re(k)}$, the actual rotor position can be changed by the load torque. If the load torque is lower than the previous step, then the actual rotor position is moved to $\theta_{r(k)}$ to decrease the torque angle. Otherwise, torque angle $\theta_{tm(k)}$ is made higher than the previous torque angle $\theta_{tm(k-1)}$ to increase the output torque.

In the proposed method, the torque angle is automatically changed in accordance with the load condition to balance the load variation. The average speed is nearly the same as the reference speed. However, the maximum output torque is limited by the magnitude of the current vector.

In the normal-speed control mode, rotor position can be derived by the hall sensor signal and the measured rotor speed. However, in the low-speed region, torque current is controlled by the torque angle between the reference current angle and the practically measured rotor position at the changing point of the hall sensor signal.

$$\widehat{\theta_{tm}} = \theta^*_{re} - \widehat{\theta_{re}}\,, \tag{7}$$

Then, the reference current can be derived as follows in the low-speed control mode:

$$I^*_{mL} = LMT\left|K_{ptc}\cdot\sin\left(\widehat{\theta_{tm}}\right)\right|, \tag{8}$$

where K_{ptc} is the gain of the proposed micro-stepping angle controller. When the gain K_{ptc} is set as the rated current of the motor, the maximum possible load is the rated output torque of the motor. Furthermore, a high gain can increase robustness to sudden load with a high speed ripple in the proposed mode. The reference current I^*_{mL} is limited by the maximum value to protect motor and drive and the minimum value to improve sudden load characteristics. When the sudden load is injected, the torque angle may be higher than 90°. Thus, the reference torque current is changed to keep the maximum torque angle in the low-speed control region with a fixed micro-stepping angle variation.

In the normal-speed region, the torque current is controlled by a conventional PI control scheme as follows:

$$I^*_{mH} = K_p\Delta\omega_m + K_i\int(\Delta\omega_m + K_a(I^*_{mH(k-1)} - I_{tmp}))dt\,, \tag{9}$$

where K_p and K_i are the PI controller gains. K_a is the gain of the anti-windup controller to limit the integral error by the limit value of the reference current.

Fig. 7 shows the proposed speed control scheme of BLDC motor. As shown in the figure, the proposed control scheme consists of two control modes: low- and normal-speed control modes. In the low-speed control mode, the torque current amplitude is controlled by the torque angle with the reference speed and reference rotating angle. In the normal-speed control mode, the torque current is controlled by the speed error with the estimated angle of the hall sensor.

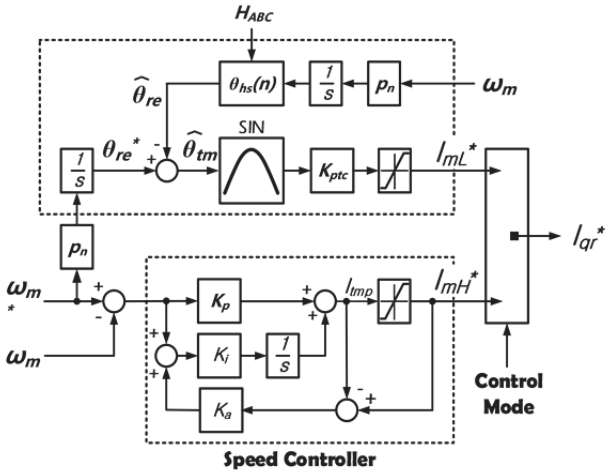

Fig. 7. Proposed speed control scheme of BLDC motor.

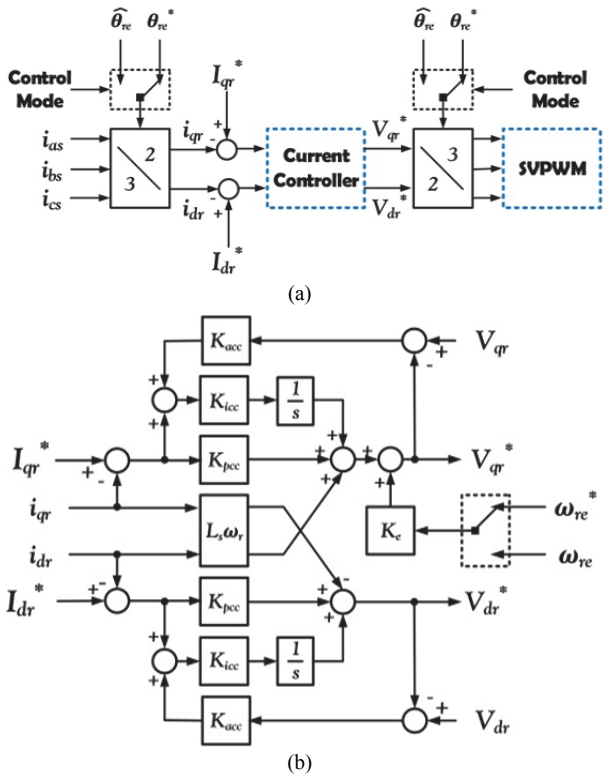

Fig. 8. Proposed current block according to the control mode. (a) Mode selectable current control block. (b) d–q axis current controller with mode selectable back EMF.

Fig. 8 shows the block diagram of the current control scheme in the proposed method. As shown in the figure, the reference micro-step angle θ^*_{re} uses d–q transformation in low-speed control mode. The estimated angle $\widehat{\theta_{re}}$ is used in the normal-speed control mode. The rotating torque current speed can be determined by the angle selection to transfer current and voltage. The current controller is designed by the anti-windup PI controller with back EMF compensation and

TABLE I
SPECIFICATIONS OF THE MOTOR

Parameters	Values	Parameters	Values
Rated Power	100 W	Voltage	24 V
Rated Speed	2000 rpm	Rated Torque	0.5 N·m
Resistance	0.35 Ω	Rated Current	6.0 A

d–q axis decoupling term. Specifically, the back EMF compensation can be done using the reference value in the low-speed control mode. The practically measured speed in the normal-speed control mode is shown in Fig. 8(b).

In the mode change, the initial reference current from low- to normal-speed mode and the initial reference angle from normal- to low-speed mode are important. To reduce the torque variation during the change in mode, the initial reference angle and current reference are calculated as follows:

$$\theta^*_{re(k)} = \theta_{re(k-1)} + sin^{-1}\left(\frac{I^*_{mL}}{I_{mH(k-1)}}\right), \quad (10)$$

$$I^*_{mH(k)} = I_{mL(k-1)} \cdot \sin(\theta_{tm(k-1)}), \quad (11)$$

IV. EXPERIMENTAL RESULTS

Experimental tests are implemented in various conditions to verify the proposed method. Table I shows the detailed specifications of the experimented BLDC motor at 24 V, 100 W rated power. Fig. 9 shows the designed BLDC motor drive based on the TMS320F28035 digital signal processor (DSP) by Texas Instruments. The phase current is measured by a chip-type current sensor and a DSP-embedded 12 bit analog-to-digital converter. The hall sensor signal of the motor is changed by the EXOR gate IC and is used to detect the actual motor speed. The current controller is designed as 64 μs with 15.625 kHz switching frequency. The rotor position of the motor is estimated by the hall sensor signals and the detected speed. Fig. 9 shows the additional load controller with torque sensor and optical encoder used to measure the practical speed and verify the speed control performance.

Fig. 10 shows the compared experimental results of the two-phase conduction method and the proposed control scheme at 20–200 rpm.

In the experiments, the current control using a micro-stepping angle is adopted at 20 rpm and the closed speed controller is adopted at 200 rpm.

As shown in Fig. 10, the control performance at the closed speed controller is nearly the same at 200 rpm. However, the practical speed of the motor cannot be controlled at 20 rpm with the conventional two-phase conduction method. The variation in the hall sensor signal frequency is serious at the 20 rpm region. Additionally, the average speed cannot follow the reference speed in Fig. 10(a). In the proposed method, the actual speed at 20 rpm can keep up with the reference speed with the sinusoidal current of micro-stepping. As shown in Fig. 10(b), the continuous rotor position $\widehat{\theta_{re}}$ can be precisely estimated in the proposed method.

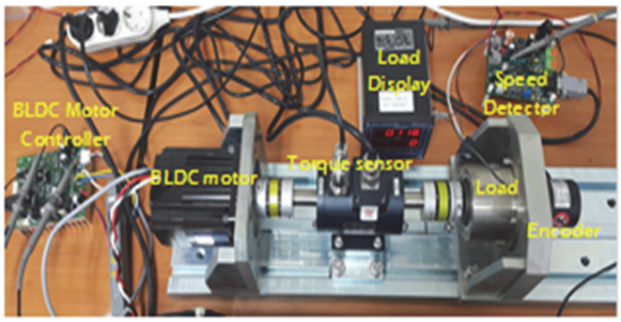

Fig. 9. Experimental configurations.

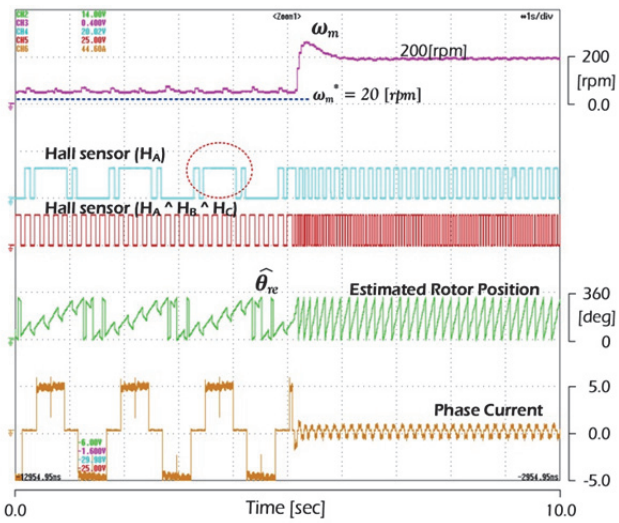

(a)

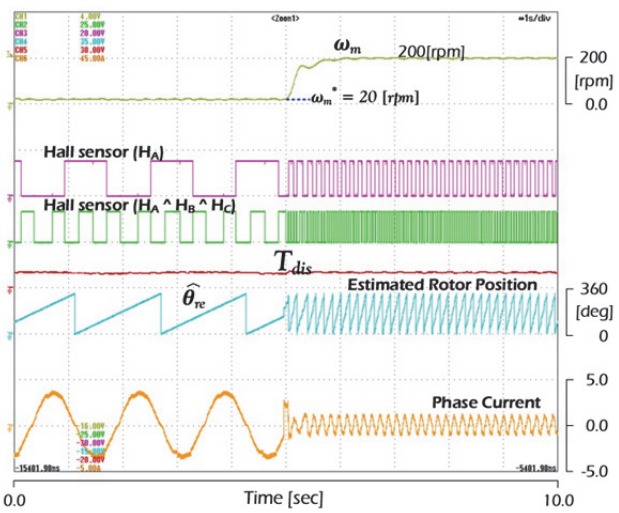

(b)

Fig. 10. Comparison of experimental results on the change in control mode. (a) Experimental result of the two-phase method (20–200 rpm). (b) Experimental result of the proposed method (20–200 rpm).

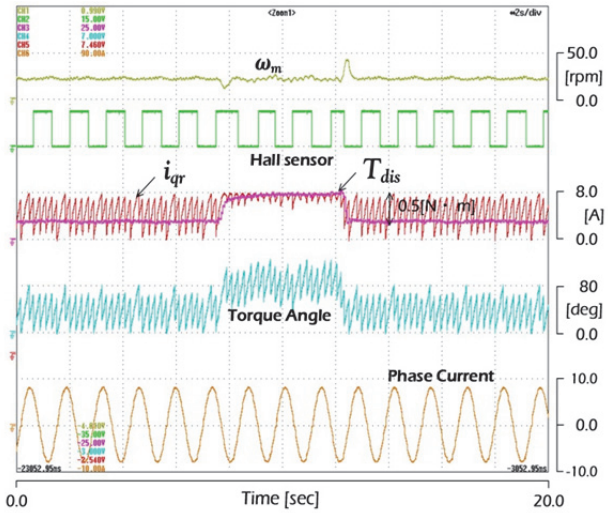

(a)

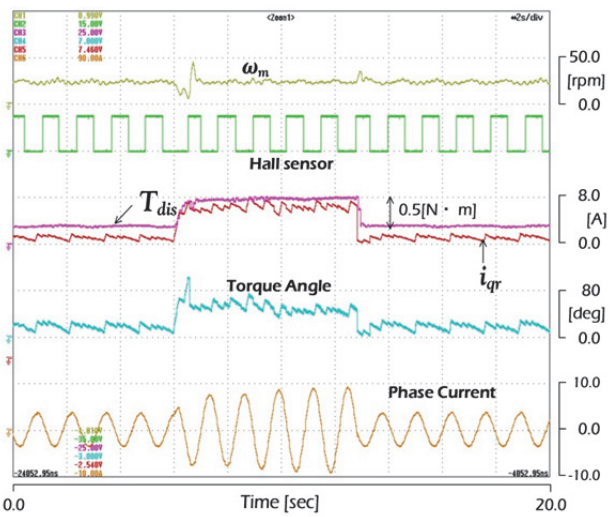

(b)

Fig. 11. Comparison of experimental results on load variation. (a) Experimental result of the constant current control (at 25 rpm). (b) Experimental result of the proposed method (25 rpm, 0.1–0.5 N·m).

Fig. 11 shows the compared experimental results at 25 rpm. In Fig. 11(a), the constant current is controlled in the micro-stepping region, and the torque angle is automatically changed in accordance with the disturbance load T_{dis} variation. The actual torque current is changed by the torque angle. In the proposed method shown in Fig. 11(b), the phase current is controlled by the estimated torque angle. At no-load condition, the phase current is decreased to the limit value, and the torque angle variation is lower than that of the constant current method. The phase current is increased according to the load variation to keep a proper torque angle in the micro-stepping mode.

Figs. 12 and 13 show the experimental results of the proposed control scheme in micro-stepping mode. In Fig. 12, the speed reference is changed from 10 rpm to 50 rpm. As shown in Fig. 12, the actual speed can keep up with the

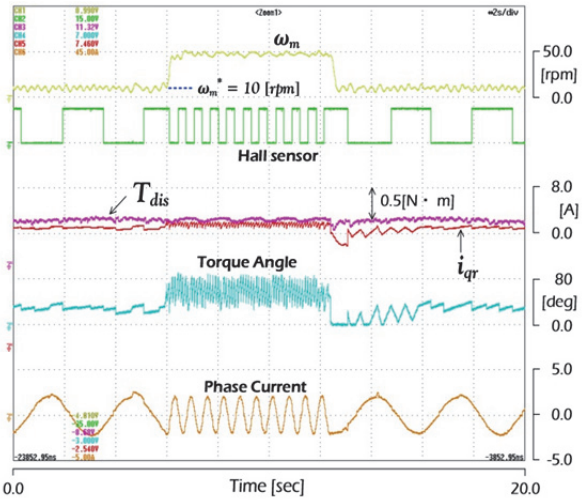

Fig. 12. Experimental result of speed variations (10–50 rpm).

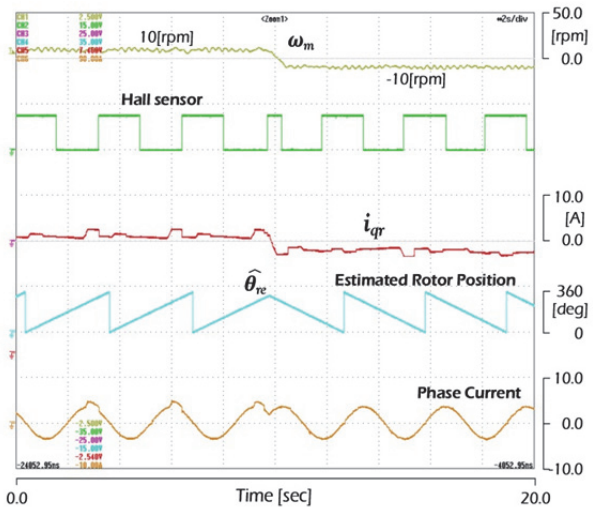

Fig. 13. Experimental result of direction changes (from 10 rpm to −10 rpm, 0.1 Nm).

reference value in the speed reference change. The phase current is determined by the load condition. In Fig. 13, the speed reference is changed from 10 rpm to −10 rpm. The actual speed of the torque sensor is measured by an optical encoder with 1024 pulses per revolution. The rotating direction can be observed from the estimated rotor position $\widehat{\theta_{re}}$ of the hall sensor signal of the motor. In Fig. 13, the actual torque current i_{qr} is calculated by the phase current and the torque angle. In negative speed, the actual torque current is negative.

As shown in Figs. 12 and 13, the motor speed can keep up well with the reference value at the speed variation in the proposed micro-stepping method.

Fig. 14 shows the experimental result of the mode changes in the proposed method. In Fig. 14, the torque angle θ_{tm} is varied in the micro-stepping mode, but it is 90° at the normal speed region due to the vector control. As shown in the figure, the speed is well controlled under the mode change.

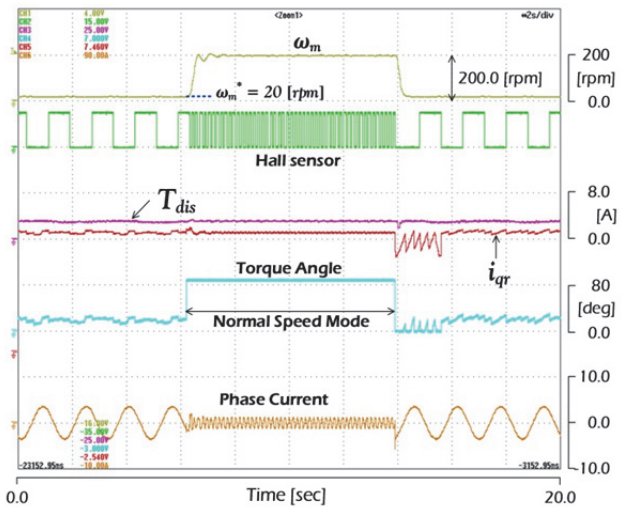

Fig. 14. Experimental result of mode changes (20–200 rpm, 0.1 N·m).

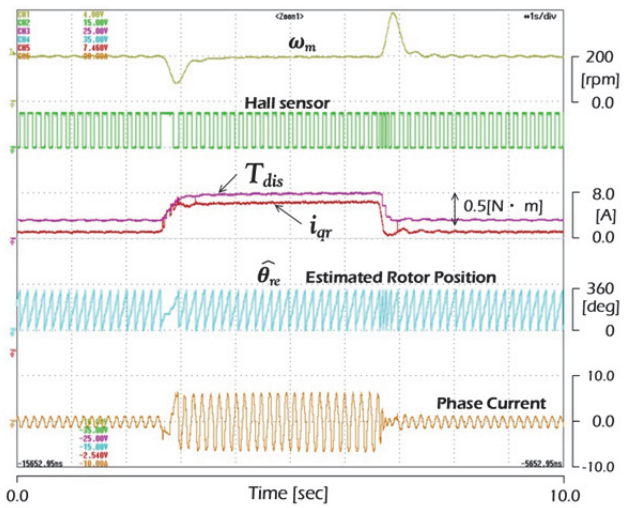

Fig. 15. Experimental result of load variations at normal mode (0.1–0.5 N·m).

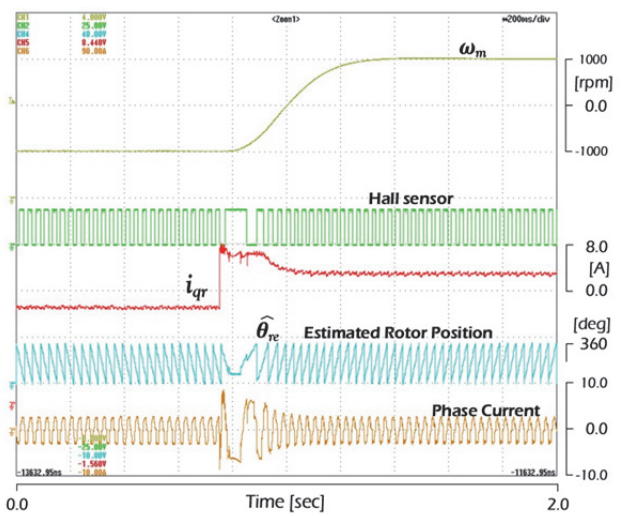

Fig. 16. Experimental result of speed variations (from −1000 rpm to 1000 rpm, 0.3 N·m).

Figs. 15 and 16 show the experimental results of the normal speed region, which is controlled by the vector control scheme. When the load is changing, the torque current is changed to keep the constant speed in the vector control mode. In Fig. 16, the reference speed is changed from −1000 rpm to 1000 rpm. As shown in the figure, the actual speed of the BLDC motor is well controlled in the vector control scheme under load variations and speed changes.

V. Conclusions

This paper presents a separated speed control scheme of BLDC motors for a wide speed range. The proposed speed control scheme exhibits a micro-step torque angle in low speed range and the vector torque control with the continuous estimated rotor position in normal speed range. The vector control of the BLDC motor is the same as the conventional control method of PMSM, except for the estimated rotor position with the hall sensor signal and detected speed.

The proposed torque angle control for the low-speed region uses the micro-step rotating current vector with the reference speed and the control of current magnitude to keep a suitable torque angle without speed feedback. The torque angle is controlled by the reference current vector and the actual detected angle from the hall sensor.

Experimental results indicate that the proposed method shows advanced performance in the low-speed region. The proposed method can keep up with the reference speed at various load conditions.

Acknowledgment

This research was supported by The Leading Human Resource Training Program of Regional Neo Industry through the National Research Foundation of Korea and funded by the Ministry of Science, ICT, and future Planning (NRF-2016H1D5A1910536) and "Human Resources Program in Energy Technology" of the Korea Institute of Energy Technology Evaluation and Planning (KETEP), granted financial resource from the Ministry of Trade, Industry & Energy, Republic of Korea. (No. 20164010200940).

References

[1] B. G. Gu, J. H. Choi, and I. S. Jung, "Simple lead angle adjustment method for brushless DC motors," *J. Power Electron.*, Vol. 14, No. 3, pp. 541-548, May 2014.

[2] C. Xia, Y. Xiao, W. Chen, and T. Shi, "Torque ripple reduction in brushless DC drives based on reference current optimization using integral variable structure control," *IEEE Trans. Ind. Electron.*, Vol. 61, No. 2, pp. 738-752, Feb. 2014.

[3] T. Shi, Y. Cao, G. Jiang, X. Li, and C. Xia, "A torque control strategy for torque ripple reduction of brushless DC motor with nonideal back electromotive force," *IEEE*

Trans. Ind. Electron., Vol. 64, No. 6, pp. 4423-4433, Jun. 2017.

[4] J. Fang, H. T. Li, and B. L. Han, "Torque ripple reduction in BLDC torque motor with non-ideal back EMF," *IEEE Trans. Power Electron*., Vol. 27, No. 11, pp. 4630-4637, Nov. 2012.

[5] C. Xia, B. Ji, and Y. Yan, "Smooth speed control for low-speed high-torque permanent-magnet synchronous motor using proportional-integral-resonant controller," *IEEE Trans. Ind. Electron*., Vol. 62, No. 4, pp. 2123-2134, Apr. 2015.

[6] M. Bertoluzzo, G. Buja, R. K. Keshri, and R. Menis, "Sinusoidal versus square-wave current supply of PM brushless DC drives: A convenience analysis," *IEEE Trans. Ind. Electron.*, Vol. 62, No. 12, pp. 7339-7349, Dec. 2015.

[7] I. Boldea and S. A. Nasar, "Torque vector control (TVC) – A class of fast and robust torque, speed and position digital controllers for electric drives," *Electric Machines & Power Systems*, Vol. 15, No. 3, pp. 135-147, 1988.

[8] F. G. Capponi, G. D. Donato, L. D. Ferraro, O. Honorati, M. C. Harke, and R. D. Lorenz, "AC brushless drive with low-resolution hall-effect sensors for surface-mounted PM machines," *IEEE Trans. Ind. Appl*., Vol. 42, No. 2, pp. 526-535, Mar./Apr. 2006.

[9] Y. Liu, J. Zhao, M. Xia, and H. Luo, "Model reference adaptive control-based speed control of brushless DC motors with low-resolution hall-effect sensors," *IEEE Trans. Power Electron*., Vol. 29, No. 3, pp. 1514-1522, Mar. 2014.

[10] J. Bernat and S. Stepien, "The adaptive speed controller for the BLDC motor using MRAC technique," *Proc. the 18th World Congress The Internaltional Federation of Automatic Control*, pp. 4143-4148, 2011.

[11] A. Darba, F. D. Belie, P. D'haese, and J. A. Melkebeek, "Improved dynamic behavior in BLDC drives using model predictive speed and current control," IEEE Trans. Ind. Electron., Vol. 63, No. 2, pp. 728-740, Feb. 2016.

[12] S. M. Yang, F. C. Lin, and M. T. Chen, "Micro-stepping control of a two-phase linear stepping motor with three-phase VSI inverter for high-speed applications," *IEEE Trans. Ind. Appl*., Vol. 40, No. 5, pp. 1257-1264, Sep./Oct. 2004.

Dong-Hee Lee was born on November 11, 1970 and received his B.S., M.S., and Ph.D. degrees in Electrical Engineering from Pusan National University, Busan, Korea, in 1996, 1998, and 2001, respectively. He worked as a senior researcher of the Servo R&D Team at OTIS-LG from 2002 to 2005. Since 2005, he has been with Kyungsung University, Busan, Korea, as a professor in the Department of Mechatronics Engineering. His major research field is the servo system and electrical motor drive with power electronics. He is an associate editor of the Journal of Power Electronics.